Supplementary information

Core-Shell Ru/NiO_x@graphene Composite Aerogel as efficient Bifunctional Electrocatalysts for Overall Water Splitting

Jiangcheng Zhang, Hu Yao, Xiayu Wang, Xin Yu, Qiuhan Cao, Xiaoyi Dong, Xiaohui Guo*

*Key Lab of Synthetic and Natural Functional Molecule Chemistry of Ministry of Education, The College of Chemistry and Materials Science, Northwest University, Xi'an 710069, P. R. China.

*Corresponding author e-mail: guoxh2009@nwu.edu.cn;

Experimental Procedure

Chemicals.

All reagents were used as purchased without further purification. Carbon paper (CP), Ruthenium chloride ($RuCl_3 \cdot xH_2O$), Nickel chloride ($NiCl_2 \cdot 6H_2O$), graphene oxide (GO), potassium hydroxide (KOH) and anhydrous ethanol (C_2H_6O) were purchased from Aladdin's Reagent. were purchased from Aladdin reagent.

Characterization

The morphology of different samples was characterized by scanning electron microscopy (SEM, SU-8010), and the morphology, structure and elemental composition and distribution of Ru/NiO_x@GA were analysed by transmission electron microscopy (TEM, Talos-200) and EDX mapping. The crystal structures of the different samples were characterised using a wide-angle X-ray powder diffractometer (XRD, Bruker D8 ADVANCE) (Cu K_α radiation) at a scanning rate of $0.05°s^{-1}$. Translated with DeepL.com (free version) The elemental composition and valence states of the samples were analysed by X-ray photoelectron spectroscopy (XPS, Thermo Scientific, ESCALAB Xi^+) with an Al K_α X-ray source.

Electrochemical measurements

All electrochemical measurements were performed at an electrochemical

workstation (CHI 660E, Inc., Shanghai, China). The various properties of the electrocatalysts were measured by a three-electrode system in 1 M KOH solution. A standard Ag/AgCl electrode and a platinum sheet were used as reference and counter electrodes, respectively. The working electrode was a carbon paper loaded with the catalyst, which was prepared as follows: Firstly, 5 mg of the sample was dispersed into a mixed solution consisting of 50 μL of Nafion (5 wt%) and 950 μL of ethanol, which was ultrasonicated for 1 h to make a homogeneous mixture. Then, 30 μL of the solution obtained in the previous step was added dropwise onto CP (1*0.5 cm^2) and dried naturally. The catalyst loading on CP was about 0.3 mg cm^{-2}. The performances of HER and OER were measured in an electrolyte of 1.0 M KOH to evaluate their electrocatalytic activities. The reference electrode was converted to RHE according to the Nernst equation ($E_{RHE}=E_{Ag/AgCl}+0.0591pH+ E_{(Ag/AgCl)}$).

Electrocatalytic performance testing

The samples were firstly activated by cyclic voltammetry (CV) at a sweep rate of 50 mV s^{-1}, and secondly, the samples were determined by linear scanning voltammetry (LSV) (with a sweep rate of 5 mV s^{-1}) at a 10 mA cm^{-2} current density of the overpotential. The electrochemical specific surface area (ECSA) of different catalysts was determined by the CV method at different scan rates from 10 to 50 mV s^{-1} and the corresponding double layer capacitance(C_{dl}) values were calculated from the ECSA. Finally, cyclic stability tests were carried out under constant current conditions (10 mA cm^{-2}). The Electrochemical impedance spectroscopy (EIS) was measured over a

frequency range of 0.01~ 10^6 Hz.

Overall water splitting test

The overall water splitting performance of the prepared catalyst was evaluted in a twoelectrode setup with the catalyst as both the anode and cathode. The carbon paper (1×0.5 cm^{-2}) with catalyst loading of 0.3 mg cm^{-2} was served as the working electrode. The polarization curves were recorded at a scan rate of 5 mV s^{-1}. The voltage range was fixed at 1.0 to 2.0 V. The durability test was conducted at a constant current density at 10 mA cm^{-2}. The performance of overall water splitting cells assembled by RuO_2//Pt/C pair were also evaluated as reference.

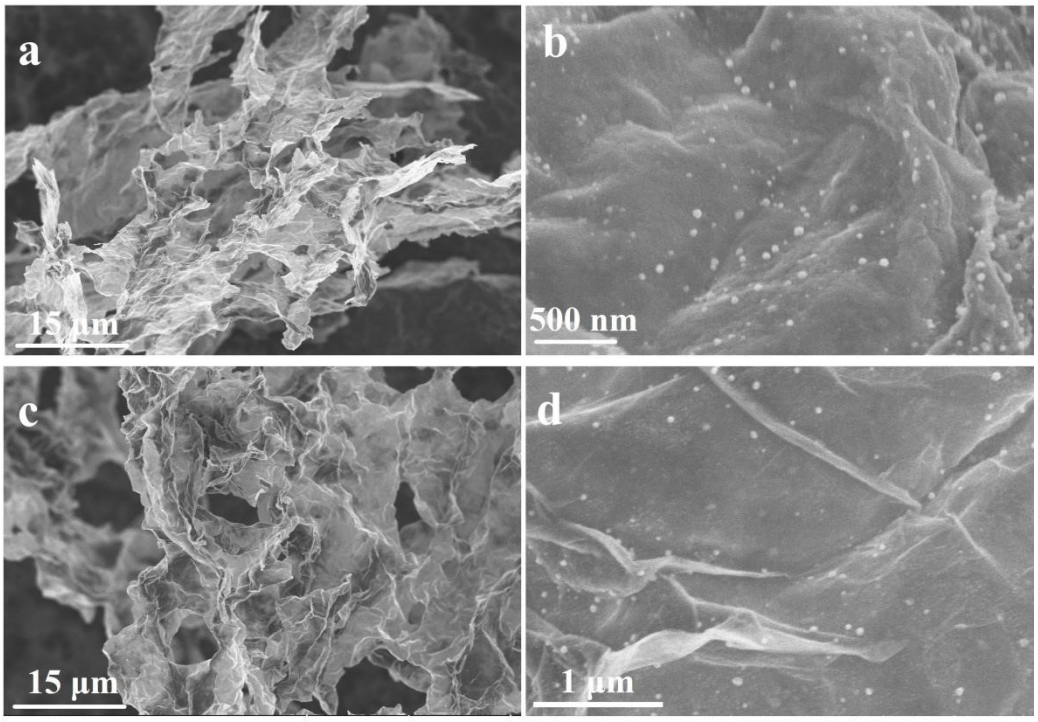

Fig. S1. SEM images of (a-b) Ru/NiO_x@GA and (c-d) Ru/Ni@GA-H with different magnifications.

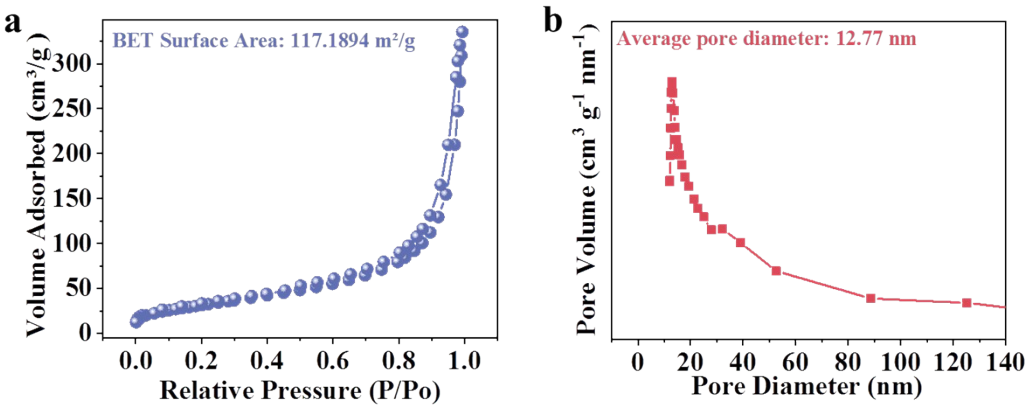

Fig. S2. (a) N_2 adsorption-desorption isotherms and (b) Pore size

distributions of the Ru/NiO_x@GA.

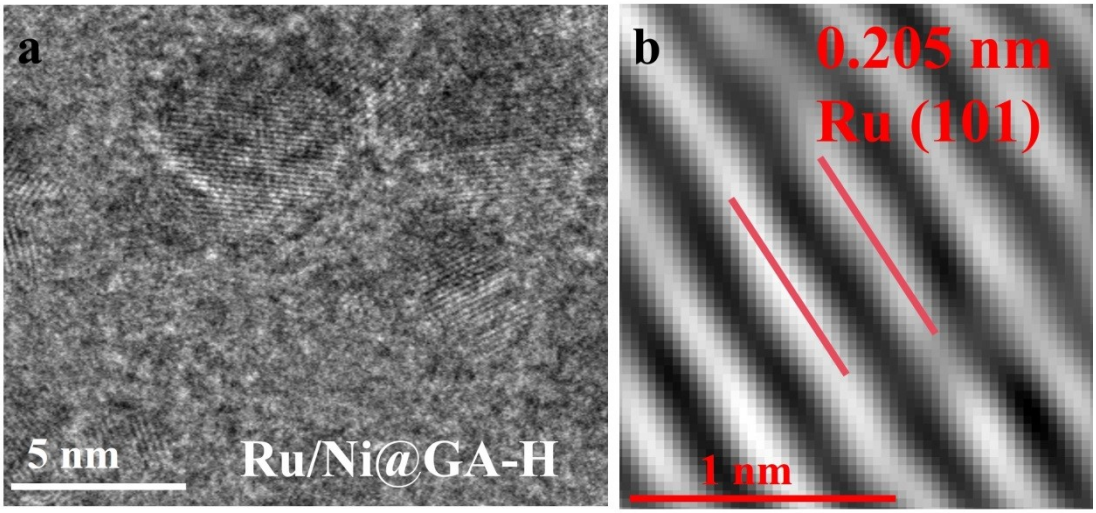

Fig. S3. (a-b) HRTEM and FFT image of Ru/Ni@GA-H.

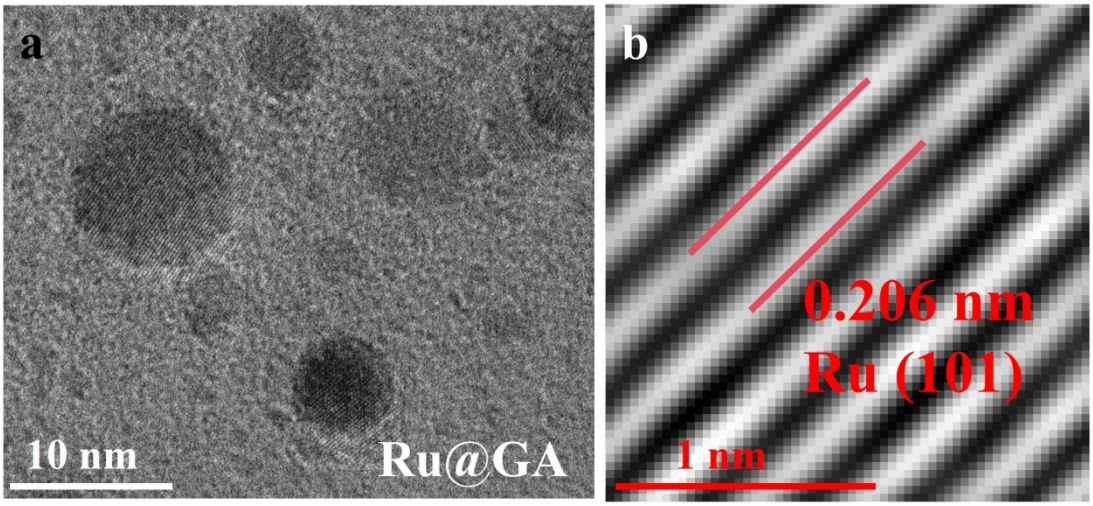

Fig. S4. (a-b) HRTEM and FFT image of Ru@GA.

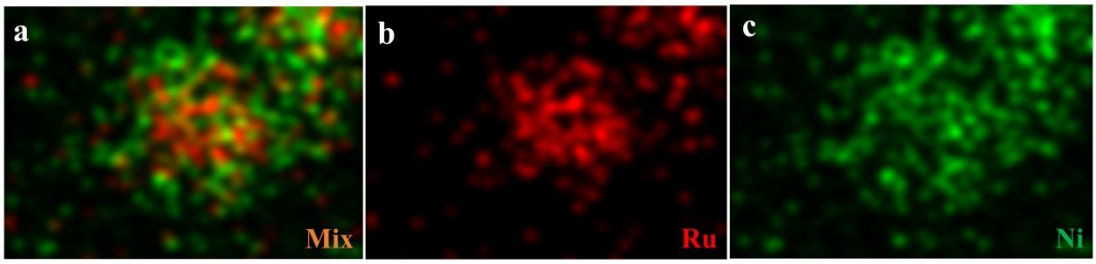

Fig. S5. EDX mapping of Ru/Ni@GA-H.

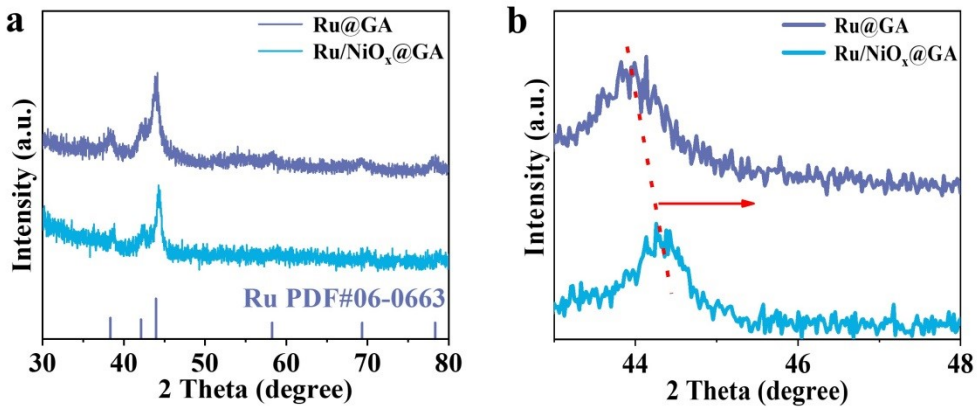

Fig. S6. (a-b) XRD patterns of Ru@GA and Ru/NiO_x@GA.

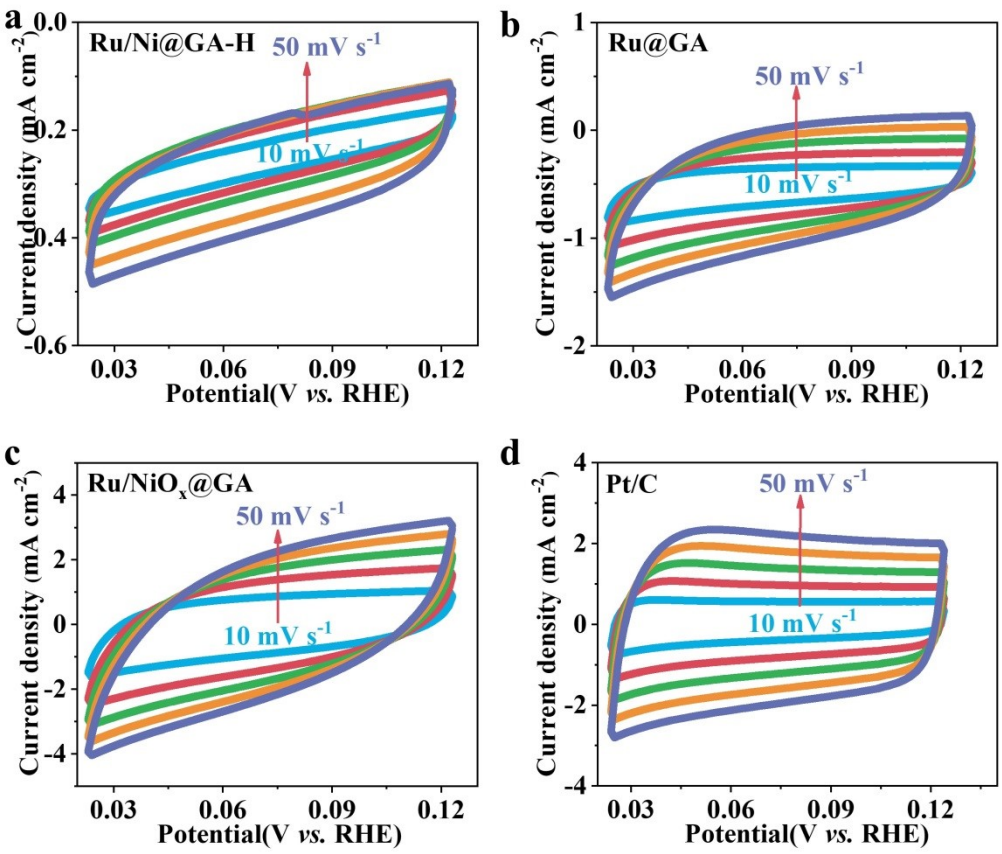

Fig. S7. cyclic voltammetry curves of (a) Ru/Ni@GA-H; (b) Ru@GA ; (c) Ru/NiO_x@GA; (d)Pt/C at different sweep speeds.

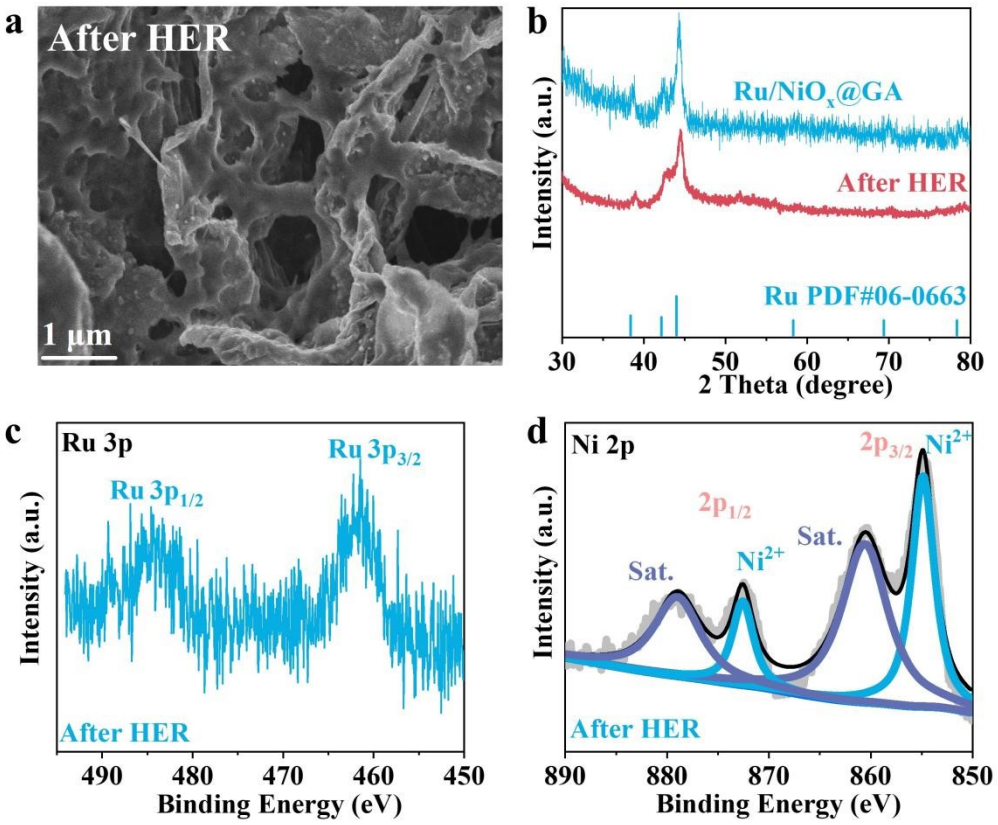

Fig. S8. (a)SEM image; (b) XRD pattern of Ru/NiO_x@GA; (c) Ru 3p; (d) Ni 2p for Ru/NiO_x@GA after 200h HER reaction.

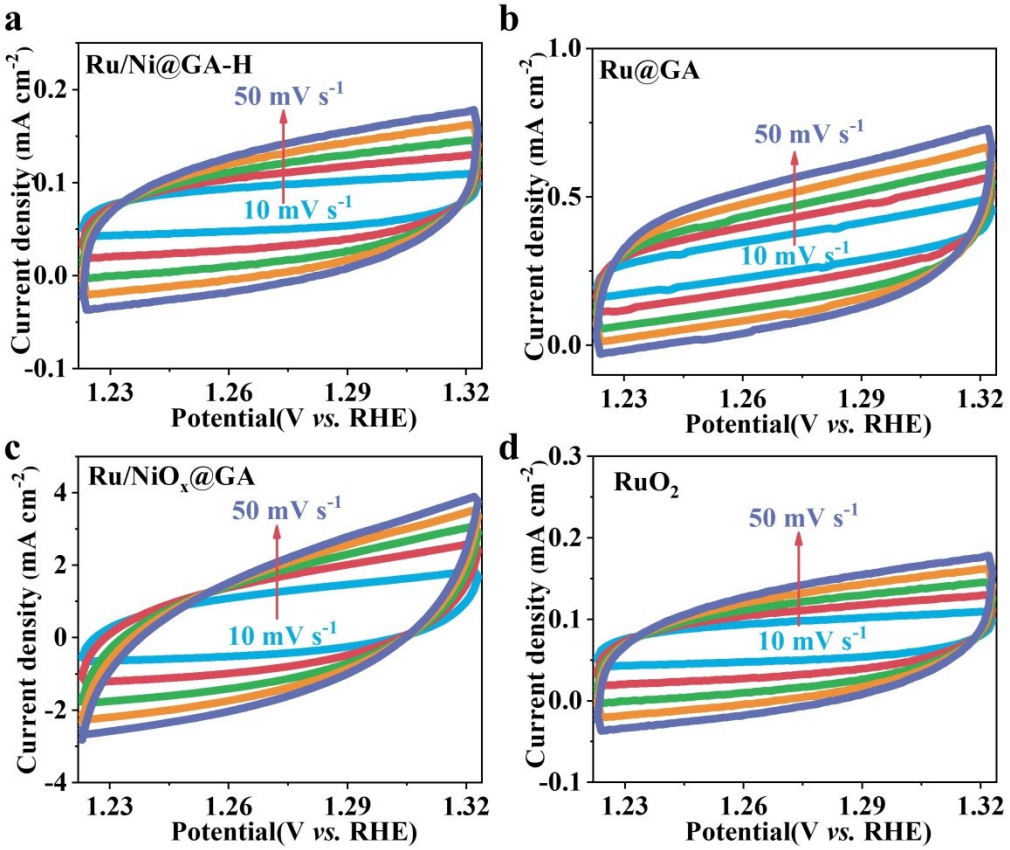

Fig. S9. OER cyclic voltammetry curves of (a) Ru/Ni@GA-H; (b) Ru@GA ; (c) Ru/NiO_x@GA; (d)RuO_2 at different sweep speeds

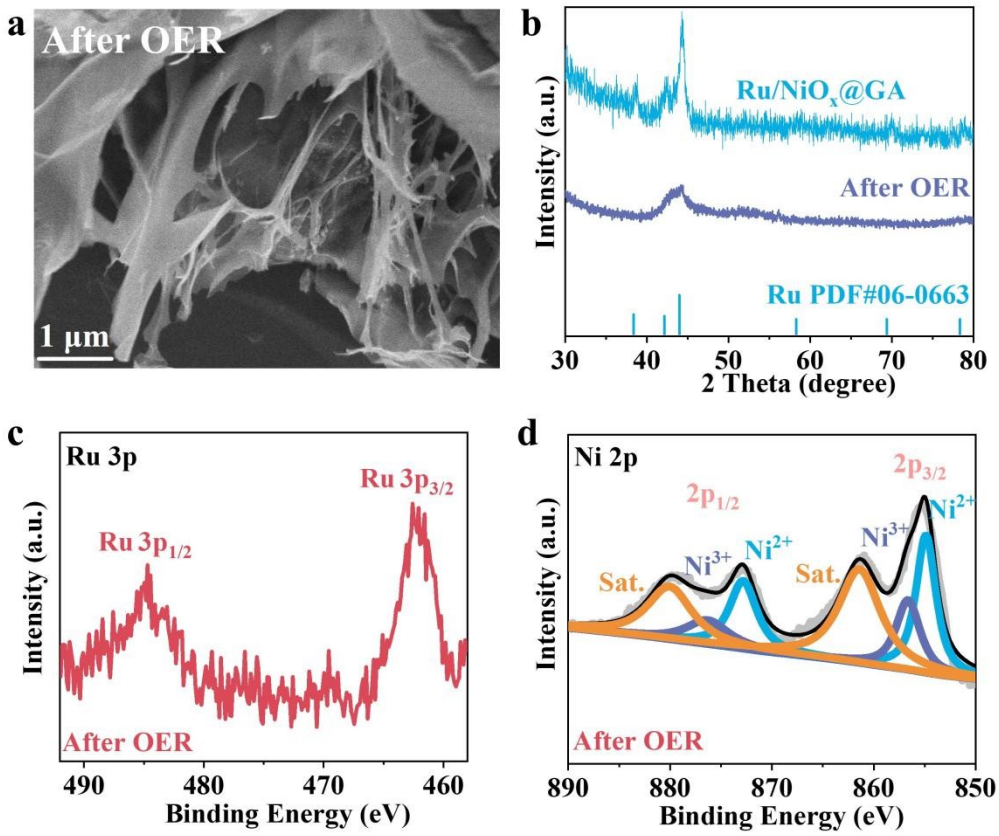

Fig. S10. (a)SEM image; (b) XRD pattern of Ru/NiO$_x$@GA; (c) Ru 3p; (d) Ni 2p of Ru/NiO$_x$@GA after 200h OER reaction.

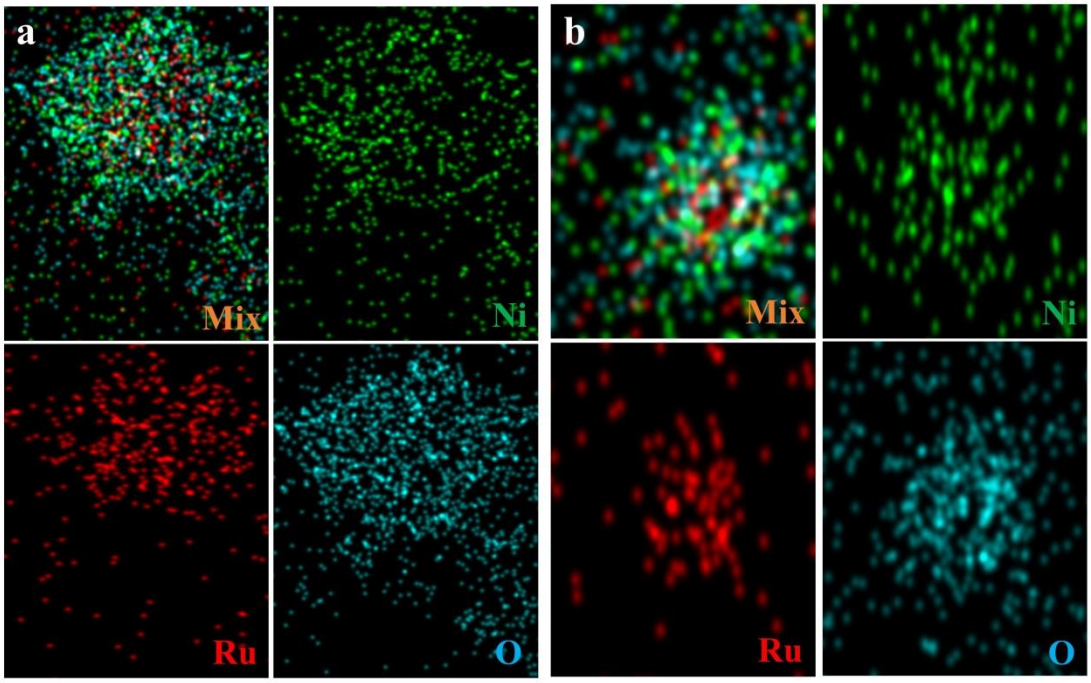

Fig. S11 EDX mapping image after long-cycle testing for (a) HER and (b) OER.

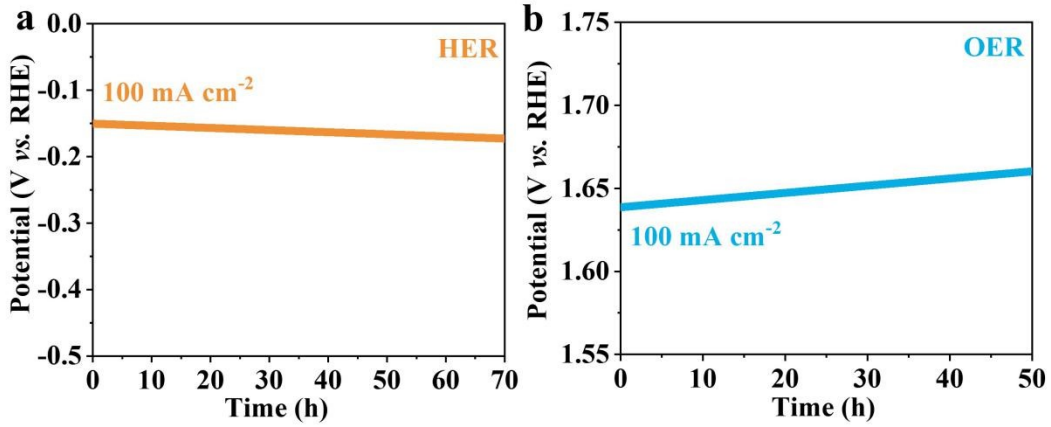

Fig. S12 Ru/NiO_x@GA at 100 mA cm^{-2} current density cycling stability for (a) HER and (b) OER.

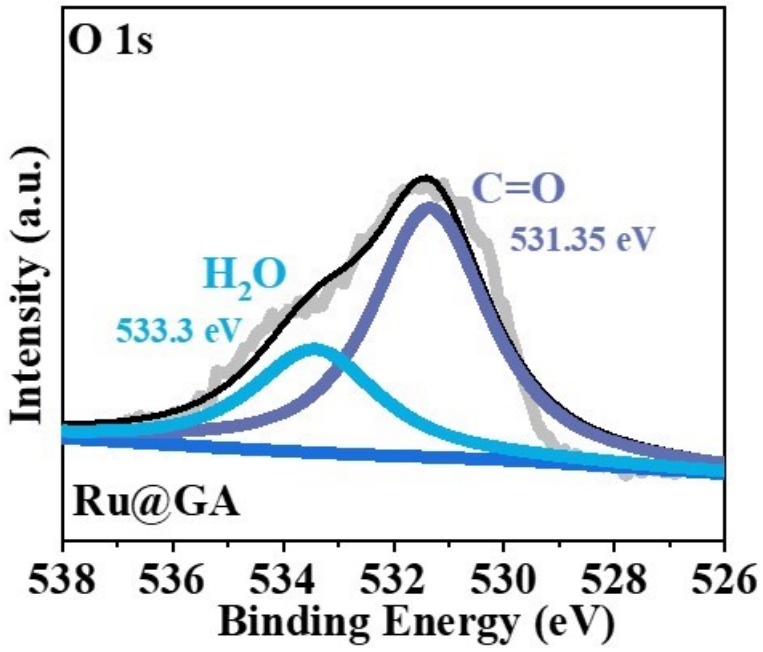

Fig. S13. O 1s XPS of Ru@GA.

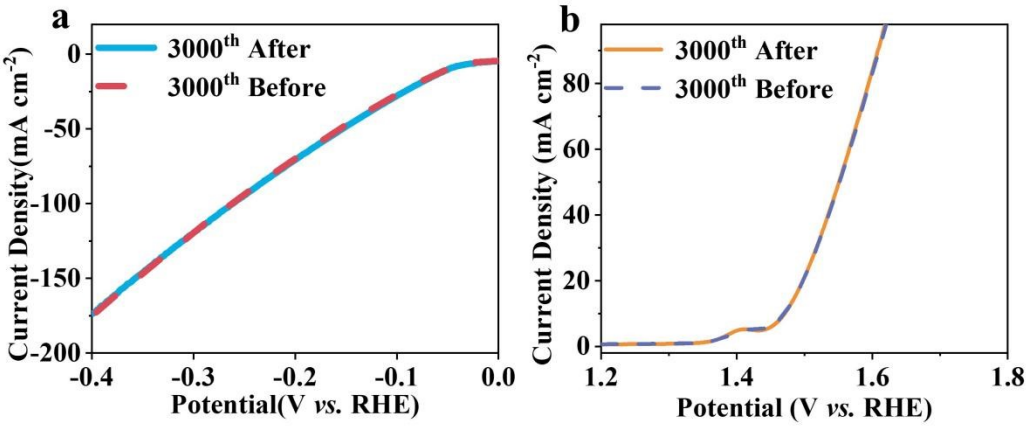

Fig. S14. Polarization curves before and after 3000 cycles of (a) HER; (b) OER.

Table S1. Impedance parameter values obtained by fitting the Nyquist curve of the equivalent circuit in HER

Samples	R_1	R_s	R_{ct}
Ru@GA	0.677	2.93	17.08
Ru/NiO_x@GA	0.680	2.458	4.554
Ru/Ni@GA-H	0.857	3.652	23.54

Pt/C	0.72	2.286	5.112

Table S2. Impedance parameter values obtained by fitting the Nyquist curve of the equivalent circuit in OER

Samples	**R_1**	**R_s**	**R_{ct}**
Ru@GA	0.89	2.122	15.24
Ru/NiO_x@GA	0.708	2.547	6.459
Ru/Ni@GA-H	0.945	2.864	132.72
RuO_2	0.787	2.862	117.85

Table S3. Comparison of the HER performance of our work with various related electrocatalysts at a current density of 10 mA cm^{-2}.

Catalyst	η_{-10} mA cm^{-2} (mV)	Tafel slope (mV dec^{-1})	Reference
CNT-V-Fe-Ru	64	51	1
Ru_n-Ru_s-NC	37	48	2
M-Co@Ru/NC	34	55	3
NiO/Ru@Ni	39	75	4
CoRu@NC	45	66	5
RuP_2@NPC	52	69	6
Ru@B,N-CNTs	54	90	7
Ni_3N/Ru/NCAC	42	59	8
Ru/NiO_x@GA	32	47.26	This work

Table S4. Comparison of the OER performance of our work with various related electrocatalysts at a current density of 10 mA cm^{-2}.

Catalyst	η_{10} mA cm^{-2} (mV)	Tafel slope (mV dec^{-1})	Reference
Ru/Co–N–C-800 °C	276	65.7	9
CoFeP@Ru	340	58	10
Ru@B,N-CNTs	315	61.5	7
Ru-FeRu@C/NC	345	64.7	11
CoNG/Ru	350	82.3	12
RuO_2/Co_3O_4	305	69	13
rGO/Ni_2P	283	43.6	14
Ru-Co_2P@Ru-N-C	280	61	15
CoP/Ti_3C_2 MXene	280	95.4	16
Ru/NiO_x@GA	237	25.3	This work

Table S5. Comparison of Total Water Decomposition Performance of our work with Various Relevant Electrocatalysts at a Current Density of 10 mA cm^{-2}.

Catalyst	η_{10} mA cm^{-2} (V)	Reference
NiFeRu-LDH/NF	1.52	[17]
Ru_1Co_yNPs	1.59	[18]
RuCoP@CN	1.60	[19]
Ru@B,N-CNTs	1.570	[7]
Ru-FeRu@C/NC	1.630	[11]
CoNG/Ru	1.580	[12]
e-$Ni_{0.6}Ru_{0.4}$@C	1.520	[20]
RuO_2-Fe_2O_3/HrGO NSs	1.860	[21]
Ru/NiO_x@GA	1.53	This work

Table S6. ICP results of Ru/NiO_x@GA

Sample Number	test element	Co（mg/L)	C1（mg/L)	Ru content (%)
Ru/NiO_x@GA	Ru	0.023	0.023	12
		0.025	0.025	
		0.025	0.025	

Table S7. The release of Ru to the solution after water splitting

Sample Number	test element	C_o（μg/L)	C_1（μg/L)
solution after water splitting	Ru	0.054	0.541
		0.058	0.581
		0.054	0.546

References

[1] T. Gao, X. Tang, X. Li, S. Wu, S. Yu, P. Li, D. Xiao, Z. Jin, Understanding the Atomic and Defective Interface Effect on Ruthenium Clusters for the Hydrogen Evolution Reaction. Acs Catal 2023, 13 (1), 49-59.

[2] C. Yang, Z. Wu, Z. Zhao, Y. Gao, T. Ma, C. He, C. Wu, X. Liu, X. Luo, S. Li, C. Cheng, C. Zhao, Electronic Structure-Dependent Water-Dissociation Pathways of Ruthenium-Based Catalysts in Alkaline H-Evolution. Small 2023, 19 (14), 2206949.

[3] H. Zhang, H. Su, M. Soldatov, Y. Li, X. Zhao, M. Liu, W. Zhou, X. Zhang, X. Sun, Y. Xu, P. Yao, S. Wei, Q. Liu, Dynamic Co-Ru Bond Shrinkage at Atomically Dispersed Ru Sites for Alkaline Hydrogen Evolution Reaction. Small 2021, 17 (49), 2105231.

[4] C. Zhong, Q. Zhou, S. Li, L. Cao, J. Li, Z. Shen, H. Ma, J. Liu, M. Lu, H. Zhang, Enhanced synergistic catalysis by a novel triple-phase interface design of NiO/Ru@Ni for the hydrogen evolution reaction. J Mater Chem A 2019, 7 (5), 2344-2350.

[5] Y. Xu, Y. Li, S. Yin, H. Yu, H. Xue, X. Li, H. Wang, L. Wang, Ultrathin nitrogen-doped graphitized carbon shell encapsulating CoRu bimetallic nanoparticles for enhanced electrocatalytic hydrogen evolution. Nanotechnology 2018, 29 (22), 225403.

[6] Z. Pu, I. Amiinu, Z. Kou, W. Li, S. Mu, RuP_2-Based Catalysts with Platinum-like Activity and Higher Durability for the Hydrogen Evolution Reaction at All pH Values. 2017, 56 (38), 11559-11564.

[7] M. Fan, X. Chen, M. Zhang, L. Cui, X. He, X. Zou, Highly dispersed Ru nanoclusters anchored on B,N co-doped carbon nanotubes for water splitting. Inorg Chem Front 2022, 9 (5), 968-976.

[8] X. Zhao, X. Yong, Q. Ji, Z. Yang, Y. Song, Y. Sun, Z. Cai, J. Xu, L. Li, S. Shi, F. Chen, C. Li, P. Wang, J. Baek, Controlled synthesis of highly active bifunctional electrocatalysts for overall water splitting using coal-based activated carbons. J Mater Chem A 2023, 11 (24), 12726-12734.

[9] C. Rong, X. Shen, Y. Wang, L. Thomsen, T. Zhao, Y. Li, X. Lu, R. Amal, C. Zhao, Electronic Structure Engineering of Single-Atom Ru Sites via Co-N4 Sites for Bifunctional pH-Universal Water Splitting. Advanced Materials 2022, 34 (21), 2110103.

[10] S. Liu, X. Mu, P. Ji, Y. Lv, L. Wang, Q. Zhou, C. Y. Chen, S. Mu, Constructing a Rod-like CoFeP@Ru Heterostructure with Additive Active Sites for Water Splitting. Chemcatchem 2020, 12 (20), 5149-5155.

[11] W. Feng, Y. Feng, J. Chen, H. Wang, Y. Hu, T. Luo, C. Yuan, L. Cao, L. Feng, J. Huang, Interfacial electronic engineering of Ru/FeRu nanoparticles as efficient trifunctional electrocatalyst for overall water splitting and Zn-air battery. Chem Eng J 2022, 437.

[12] T. He, Y. Peng, Q. Jia, J. Lu, Q. Liu, R. Mercado, Y. Chen, F. Nichols, Y. Zhang, S. Chen, Nanocomposites Based on Ruthenium Nanoparticles Supported on Cobalt and Nitrogen-Codoped Graphene Nanosheets as Bifunctional Catalysts for Electrochemical Water Splitting. Acs Appl Mater Inter 2019, 11 (50), 46912-46919.

[13] H. Liu, G. Xia, R. Zhang, P. Jiang, J. Chen, Q. Chen, MOF-derived RuO/CoO heterojunctions as highly efficient bifunctional electrocatalysts for HER and OER in alkaline solutions. Rsc Adv 2017, 7 (7), 3686-3694.

[14] P. Li, R. Chen, S. Tian, Y. Xiong, Efficient Oxygen Evolution Catalysis Triggered by Nickel Phosphide Nanoparticles Compositing with Reduced Graphene Oxide with Controlled Architecture. Acs Sustain Chem Eng 2019, 7 (10), 9566-9573.

[15] P. Wang, K. Wang,Y. Liu, H. Li, Y. Guo, Y. Tian, S. Guo, M. Luo, Y. He, Z. Liu, S. Guo, Dual-Type Ru Atomic Sites for Efficient Alkaline Overall Water Splitting. Adv Funct Mater 2024, 34 (36), 2316709.

[16] L. Yan, B. Zhang, S. Wu, J. Yu, A general approach to the synthesis of transition metal phosphide nanoarrays on MXene nanosheets for pH-universal hydrogen evolution and alkaline overall water splitting. J Mater Chem A 2020, 8 (28), 14234-14242.

[17]G. Chen, T. Wang, J. Zhang, P. Liu, H. Sun, X. Zhuang, M. Chen, X. Feng, Accelerated Hydrogen Evolution Kinetics on NiFe-Layered Double Hydroxide Electrocatalysts by Tailoring Water Dissociation Active Sites. Advanced Materials 2018, 30 (10), 1706279.

[18]Y. Bao, J. Dai, J. Zhao, Y. Wu, C. Li, L. Ji, X. Zhang, F. Yang, Modulation in Ruthenium-Cobalt Electronic Structure for Highly Efficient Overall Water Splitting. Acs Appl Energ Mater 2020, 3 (2), 1869-1874.

[19]B. Yang, Y. Du, M. Shao, D. Bin, Q. Zhao, Y. Xu, B. Liu, H. Lu, MOF-derived RuCoP nanoparticles-embedded nitrogen-doped polyhedron carbon composite for enhanced water splitting in alkaline media. Journal of Colloid and Interface Science 2022, 616, 803-812.

[20]Q. Yang, P. Jin, B. Liu, L. Zhao, J. Cai, Z. Wei, S. Zuo, J. Zhang, L. Feng, Ultrafine carbon encapsulated NiRu alloys as bifunctional electrocatalysts for boosting overall water splitting: morphological and electronic modulation through minor Ru alloying. J Mater Chem A 2020, 8 (18), 9049-9057.

[21]H. Mosallaei, H. Hadadzadeh, A. Ensafi, K. Mousaabadi, M. Weil, A. Foelske, M. Sauer, Evaluation of HER and OER electrocatalytic activity over RuO-FeO nanocomposite deposited on HrGO nanosheets. International Journal of Hydrogen Energy 2023, 48 (5), 1813-1830.